J Surfact Deterg (2020)
DOI 10.1002/jsde.12379

ORIGINAL ARTICLE

Nonionic Isatin Surfactants: Synthesis, Quantum Chemical Calculations, ADMET and Their Antimicrobial Activities

Ahmed M. Hussein[1,2] · **Manal M. Khowdiary**[3]

Received: 25 February 2018 / Revised: 4 September 2019 / Accepted: 16 October 2019

Abstract The most challenge task in the building up of surface-active molecules is maximizing their surface activity with good biological activity. A nonionic surfactant (*N*-isatin-EO_m-C_n where *m* is 5, 7 and 9 ethylene glycol units and *n* is 8, 10 and 12) is achieved by first reacting isatin with chloroacetic acid and then with different types of ethoxylated (C_8–C_{12}) fatty alcohols that possess 5, 7 and 9 ethylene oxide units. The prepared surfactants were characterized by FTIR and ^{1}H NMR to confirm the structure. The surface activity, biodegradability, antimicrobial, and antifungal activity of the surfactants were evaluated. In addition, quantum chemical calculations and computations of oral bioavailability were performed. The obtained data show that all the synthesized compounds had good surface activity, biodegradability and biological activity.

Keywords Biological activity-docking studies · Isatin surface-active agents · Isatin-*N*-acetic acid · Nonionic surfactants

J Surfact Deterg (2020).

Supporting information Additional supporting information may be found online in the Supporting Information section at the end of the article.

✉ Manal M. Khowdiary
manalforbank@yahoo.com

[1] Department of Chemistry, Faculty of Science, Benha University, Benha, 2740, Egypt

[2] Department of Chemistry, Faculty of Applied Science, Al-Lieth University College, Umm Al Qura University, 2307, Saudi Arabia

[3] Egyptian Petroleum Research Institute, Applied Surfactant Laboratory, Nasr City, Cairo, Egypt

Present address: Ahmed M. Hussein, Department of Chemistry, Faculty of Science, Jazan University, Jazan, Saudi Arabia.

Introduction

A nonionic surfactant is a surfactant that can be prepared by ethoxylating active hydrogen carried by fatty organic compounds using catalysts (bases, acids) (Cress, 1987), as well as unconventional catalysts (Sallay et al., 1997). The presence of a heterocyclic moiety in the structure of a surfactant molecule is an efficient method for obtaining surface-active agents, as well as providing high biological activity (Albright et al., 1981; Pegiadou-Koemtjopoulou et al., 1998). Isatin is classified as one of the most important heterocyclic compounds. It has biological activity and plays an important role in medicinal chemistry. Isatin and several isatin derivatives has reported as potential biological active drugs (Jays et al., 2011). Different types of isatin compounds have been synthesized from isatin and evaluated as effective severe acute respiratory syndrome (SARS) corona virus 3CL protease inhibitors (Chen et al., 2005).

N-substituted isatin compounds were prepared and tested as antibacterial, antifungal, and antiviral agents (Jarrahpour et al., 2007). In addition, isatin reacted with chloroacetic acid in the presence of anhydrous potassium carbonate to give *N*-isatinacetic acid. Moreover, when thionyl chloride reacted with *N*-isatinacetic acid, the result was *N*-isatinacetyl chloride (Arief et al., 2013). Additionally, *N*-hydroxymethyl isatin has been prepared by a simple method (Jancevska and Stojceva, 1975). The conditions for building up a surfactant molecule based on an isatin moiety are therefore available and can be considered.

In this work, nonionic surfactants based on isatin molecules were prepared and evaluated as surface-active agents. Fourier-transform infra red spectroscopy (FTIR)

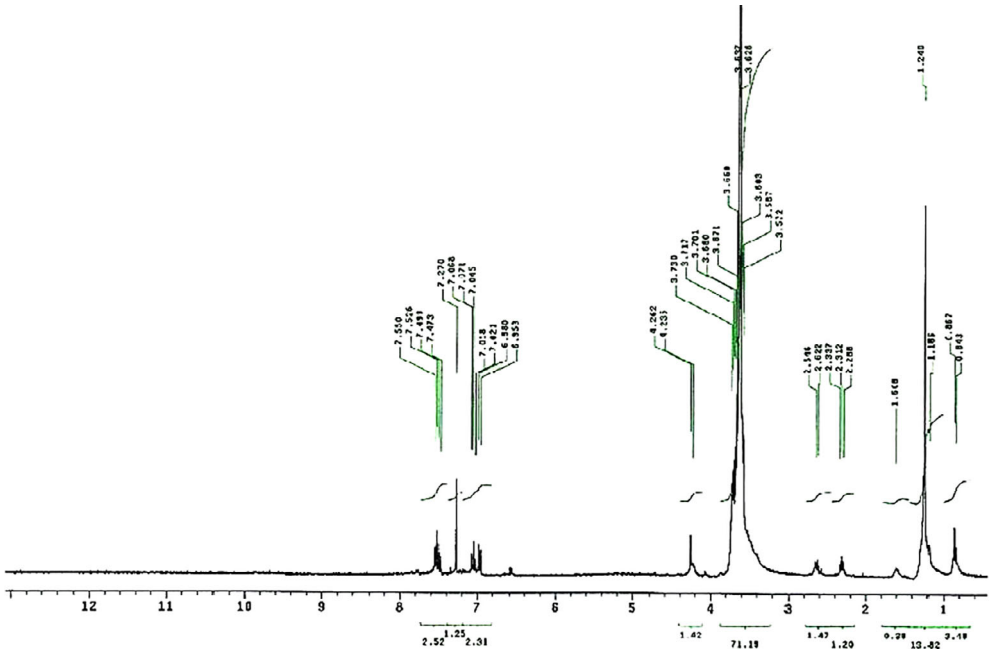

Fig. 1 [1]HNMR spectrum of compound **4c**

and Proton nuclear magnetic resonance ([1]H NMR) were used to confirm the structure of the prepared surfactants. The surface activity, biodegradability, and antimicrobial and antifungal activities were evaluated. In addition, quantum chemical calculations and computations of oral bioavailability were studied.

Experimental

Materials

Fatty alcohols (octyl alcohol, C_8, Aldrich, purity ≥98%, Cairo, Egypt; (decyl alcohol, C_{10}, Aldrich, purity ≥98%; dodecyl alcohol, C_{12}, Aldrich, purity ≥98%; tetradecyl alcohol, C_{14}, Aldrich, purity ≥97%; hexadecyl alcohol, C_{16}, Aldrich, purity ≥97%; octadecyl alcohol, C_{18}, Aldrich, purity ≥97%), ethylene oxide (Aldrich purity 99.9%), isatin (Merck purity ≥98%), chloroacetic acid and potassium carbonate (Sigma-Aldrich purity ≥98%) were utilized in this study. Solvents of acetone and toluene were fractionally distilled just prior to use. Thionyl chloride 97% (Sigma-Aldrich), thin-layer chromatography (TLC) (silica gel on a TLC, Al foil 10 cm × 20 cm, 200 μm) and molecular sieves, 4 Å, 8 mesh (Sigma-Aldrich) were also used in this investigation.

Preparation of the Nonionic Surfactants (*N*-Isatin-$EO_{5,7,9}$-$C_{8,10,12}$)

*Preparation of Isatin-*N*-Acetic Acid*

Isatin (1.74 g, 10 mmol), chloroacetic acid (0.945 g, 10 mmol), and anhydrous K_2CO_3 (1.38 g, 10 mmol) were mixing in 50 mL dry acetone and heated under reflux for 6 h. TLC was used to follow the formation of isatin-*N*-acetic acid. The solid product was separated and filtered. The product was dried under reduced pressure to give orange crystals and recrystallized from ethanol, m.p. 113–115 °C.

Preparation of Ethoxylated Fatty Alcohols

Ethoxylated fatty alcohols ($C_{8,10,12}$) were producing using a semi-micro apparatus with a K10 clay catalyst at 40–50 °C (Sallay et al., 1997). The EO was added to the reactor (free from oxygen) containing 0.1 mol fatty alcohols and about 0.2–0.55 wt% catalyst to give the desired average degree of ethoxylation (5, 7 and 9 mol of ethylene oxide) (Hussein and Khowdiary, 2014). The EO uptake (average degree of ethoxylation) was determined from the increasing weight of the reaction mixture and confirmed by IR and [1]HNMR (Ahmed et al., 1996). The reaction conditions and product characterization of the ethoxylation process are given in Table 1.

Table 1 Reaction conditions and product characterization ethoxylation process

Alcohol (mole, g)	Catalyst concentration wt% (g)	Reaction temperature (°C)	Yield %	ADE
$C_8H_{18}O$ (0.1, 13)	0.260	45	95	5, 7, 9
$C_{10}H_{22}O$ (0.1, 15.8)	0.316	45	95	5, 7, 9
$C_{12}H_{26}O$ (0.1, 18.6)	0.372	50	94	5, 7, 9
$C_{14}H_{30}O$ (0.1, 21.4)	0.428	50	93	5, 7, 9

ADE, average degree of ethoxylation.

*Preparation of the Nonionic Surfactants (*N-*Isatin-EO$_{5,7,9}$-C$_{8,10,12}$) from Reaction of Isatin*-N-*Acetic Acid with Ethoxylated Fatty Alcohols*

Isatin-*N*-acetic acid (5 mmol, 1.025 g), ethoxylated fatty alcohols (5 mmol), 50 mL dry toluene and a few drops of concentrated H_2SO_4 with molecular sieves (A° 4,8 mesh) were put into a reflux system. The reaction mixture was stirred at 150 °C for 24–36 h. The product was separated by evaporation of the reaction solvent. Table 2 shows the reaction conditions and characteristics of the prepared nonionic surfactants (*N*-isatin-EO$_{5,7,9}$-C$_{8,10,12}$), which are indicated by $(4–6)_{a–c}$.

Characterization of the Chemical Structure of the Prepared Compounds

Infera red (IR) spectra of KBr powder-pressed pellets were recorded on a Shimadzu 470 spectrometer. ^{1}HNMR spectra as shown in Fig. 1 were measured in dimethylsulfoxide (DMSO) solution using a Varian Gemini 300 (1H 300.0199481 MHz) with transcranial magnetic stimulation (TMS) as the internal standard, and the chemical shifts were reported in parts per million (ppm) on a δ-scale (Microanalytical Center and Central Laboratory, Cairo University, Egypt).

Surface Property Evaluation of the Prepared Surfactants $(4–6)_{a–c}$

Surface Tension Measurements

The surface tensions (STs) were measuring using a tensiometer K6-processor (Krüss Company, Hambrug, Germany) and the platinum ring detachment method (±0.5 mN m^{-1}) (Chavda et al., 2011).

Cloud Point

The cloud point was determined by stepwise elevation of the temperature of the prepared surfactant solution (1.0 wt % concentration). The time at which the turbidity started to form in the clear solution. This temperature was checked by reducing the solution temperature until the solution became clear again (Durham, 1961).

Table 2 Reaction conditions and product characterization of nonionic surfactants (*N*-isatin-EO$_{5,7,9}$-C$_{8,10,12}$)

Compound	Isatin-*N*-acetic acid (g, mmol)	Ethoxylated fatty alcohol (g, mmol)	Reaction time (h)	Products (g, mmol)	m.p. (°C)	Yield (%)	Color
C_8E_n							
4$_a$	(1.025, 0.005)	(1.75, 0.005)	24	(2.478, 0.0046)	189–190	92.29	Yellow
4$_b$	(1.025, 0.005)	(2.19, 0.005)	26	(2.90, 0.00456)	192–193	91.20	Yellow
4$_c$	(1.025, 0.005)	(2.63, 0.005)	30	(3.209, 0.0045)	196–197	90.01	Yellow
$C_{10}E_n$							
5$_a$	(1.025, 0.005)	(1.89, 0.005)	30	(2.543, 0.0045)	191–192	90.02	Yellow
5$_b$	(1.025, 0.005)	(2.33, 0.005)	30	(2.92, 0.00447)	196–197	89.43	Deep yellow
5$_c$	(1.025, 0.005)	(2.77, 0.005)	32	(3.15, 0.00425)	200–201	85.02	Deep yellow
$C_{12}E_n$							
6$_a$	(1.025, 0.005)	(2.03, 0.005)	35	(2.63, 0.00443)	208–210	88.70	Orange
6$_b$	(1.025, 0.005)	(2.47, 0.005)	35	(3.00, 0.00 44)	215–216	88.11	Orange
6$_c$	(1.025, 0.005)	(2.91, 0.005)	35	(3.20, 0.00416)	220–221	83.12	Orange

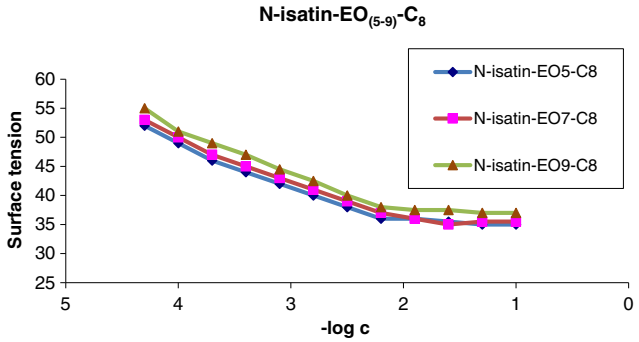

Fig. 2 Surface tension *versus* log concentration of *N*-isatin-$EO_{(5–9)}$-C_8 at 25 °C

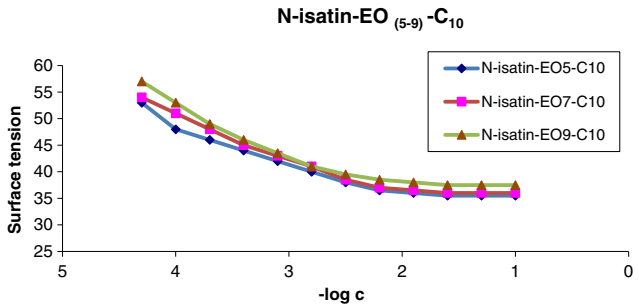

Fig. 3 Surface tension *versus* log concentration of *N*-isatin-$EO_{(5–9)}$-C_{10} at 25 °C

Foaming Height

The foaming height was measured by placing 25 mL from a solution of 0.1 g of the prepared surfactant in 100 mL water into a graduated glass cylinder. Next, the cylinder was shaken well for 10 s, the solution was allowed to settle for 30 s, and then the foam height was measured (Geng et al., 2013; Saito et al., 1989).

Wetting Time

The wetting time is the recorded time to wet cotton fabric at a 0.1 wt% aqueous surfactant solution. (Cohen and Rosen, 1981).

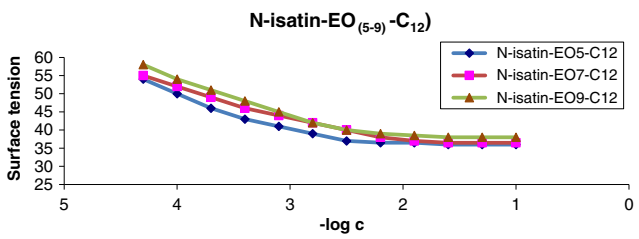

Fig. 4 Surface tension *versus* log concentration of *N*-isatin-$EO_{(5–9)}$-C_{12} at 25 °C

Biodegradability

The biodegradability was investigated by dissolving the prepared compounds in river water and measured by using a (Krüss type K6) tensiometer. Each surfactant (100 ppm) was dissolved in river water and then the samples were incubated at 38 °C. A sample was withdrawn daily (for 8 days) and filtered, and the ST value measured. The biodegradation percent (*D*%) calculated as follows:

$$D = (\gamma t - \gamma 0 / \gamma bt - \gamma 0) \times 100$$

where γ_t is the ST at the time measured, γ_0 is the ST at the starting time, and γ_{bt} is the ST of the controlling sample at the time mesured.

Measurement of the Surface Parameters

Critical Micelle Concentration

The critical micelle concentration (CMC) values for the products were measured using ST techniques and plotting the negative log of the surfactant concentration. The concentration of the surfactant *versus* the ST is shown in Figs 2–4 (Hussein and Khowdiary, 2014).

Efficiency

The efficiency (PC_{20}) is the concentration (mol L^{-1}) at which the ST is reduced by 20 dyne cm^{-1}. The PC_{20} values are measured from Figs 2–4 (Hussein and Khowdiary, 2014).

Effectiveness

The ST at CMC (γ_{cmc}) values used to calculate the values of the surface pressure (effectiveness, Πcmc) from the following expression:

$$\Pi \mathrm{cmc} = \gamma o - \gamma \mathrm{cmc}$$

where γ_o is the ST of pure water at room temperature.

Maximum Surface Excess

The maximum surface excess (Γmax) is the surface concentration at which the surfactant molecules are adsorbed at over the entire interface area. Γ_{max} is calculated from the ST using Gibb's equation (Hussein and Khowdiary, 2014):

$$\Gamma\max = \frac{1}{2.303\mathrm{RT}}\left(\frac{\delta\gamma}{\delta \log c}\right)T$$

where *R* is 8.314 J mol^{-1} K^{-1}, *T* is the absolute temperature, and ($\delta\gamma/\delta$ log*C*) is the slope of the γ *versus* log*C* plot at 25 °C.

Minimum Surface Area

The minimum surface area (A_{min}) is the minimum area per molecule of prepared compounds at the interface. A_{min} is calculated using the following equation:

$$A_{min} = \frac{10^{14}}{\Gamma_{max} * N}$$

where N is Avogadro's number and Γ_{max} is the maximum surface excess.

Molecular Modeling

The conformations of the target compounds were estimated using semiempirical molecular orbitals from the calculated energy, and geometrical optimization for the ligand structure exhibited a common feature (Tables S1–S3) and Fig. 5. The most stable conformer was fully geometrically optimized using the molecular orbital function AM1 semiempirical Hamiltonian molecular orbital calculation MOPAC 16 package, which uses the MMFF 94 (Halgren, 1996) force-field (calculations *in vacuo*, bond dipole option for electrostatics, PolakeRibiere algorithm, RMS gradient of 0.01 kcal mol^{-1}) implemented in MOE (Molecular Operating Environment, 2017).

Measurement of Antimicrobial Activity

The biological activity of the prepared compounds was measured at the Micro Analytical Center, Cairo University, Egypt. The antimicrobial activities of the tested samples were determined using a modified Kirby-Bauer disc diffusion method (Bauer et al., 1966; Liebowitz et al., 2001; Pfaller et al., 1988; Takeshita et al., 1982).

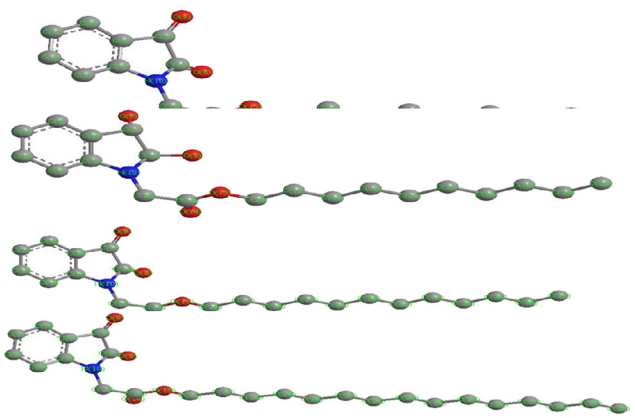

Fig. 5 Optimized for compounds $\mathbf{4}_a$, $\mathbf{5}_a$, $\mathbf{6}_a$, and $\mathbf{6}_b$ computed at semiempirical PM3

Computational Study

Preparation of Small Molecules

The target compounds were built by minimizing their energy with PM3 through MOPAC 16 then DFT using B3LYP/6-311G. All the quantum chemical computations were performed using the PM3 semi-empirical Hamiltonian molecular orbital calculation MOPAC16 package, and then employing density function theory in the Gaussian 09W program package with the Becke3-Lee-Yang-parr (B3LYP) level using 6-311G* basis as implemented in the MOE 2015 package. Optimization geometry for molecular structures was carried out to improve our knowledge of the chemical structures. Our compounds were introduced into the binding sites according to the published crystal structures.

Selection of Protein Structures

A docking experiment was carried out for the target active site into DNA Gyrase B (ID: 4uro) using MOE 2015. The errors in the active sites were corrected by the structure preparation process in MOE. After the correction, hydrogens were added and partial charges (Amber12: EHT) were calculated. Energy minimization (AMBER12: EHT, root mean square gradient: 0.100) was performed.

Binding Site Analysis

The binding site of each receptor was identified through the MOE Site Finder program, which uses a geometric approach to calculate the putative binding sites in a protein, starting from its tridimensional structure. This method is not based on energy models, but only on alpha spheres, which are a generalization of convex hulls. The prediction of the binding sites, performed by the MOE Site Finder module, confirmed the binding sites defined by the co-crystallized ligands in the holo-forms of the investigated proteins.

MOE Stepwise Docking Method

The crystal structures of the enzymes were obtained. Water and the inhibitor molecules were removed, and hydrogen atoms added. The parameters and charges were assigned with a MMFF94x force field. After alpha-site spheres generated by using the site finder module of MOE. The optimized 3D structures of molecules subjected to generate different poses of ligands by using triangular matcher placement method, which generates poses by aligning ligand triplets of atoms on triplets of alpha spheres represented in the receptor site points, a random triplet of alpha sphere center used to determine the pose during each iteration. The pose generated rescoring using the London

DG. scoring function. The poses generated refining with MMFF94x forcefield, also, the solvation effects treated. The Born solvation model (GB/VI) used to calculate the final energy, and the finally assigned poses were assigning by a score based on the free energy in kcal mol^{-1}.

Results and Discussion

Chemistry

In this work nonionic surfactants were synthesized based on an isatin nucleus, which can react with chloroacetic acid (Arief et al., 2013) to give isatin-*N*-acetic acid, and esterified with different ethoxylated fatty alcohols ($C_{8,10,12}$) with 5, 7 and 9 mol of ethylene glycol units to provide nonionic surfactants (*N*-isatin-$EO_{5,7,9}$-$C_{8,10,12}$ which abbreviated by 4–$6_{a–c}$) (Scheme 1). The chemical structures of the novel nonionic surfactants were confirmed by FTIR spectra (Table 3) and proton magnetic resonance data (Fig. 1 and Table 4).

Surface Properties of the Prepared Surfactants

The surface properties (cloud, foaming power, and wetting power) of the aqueous solutions of the prepared nonionic surfactants in a neutral medium were measured and tabulated as shown in Table 5.

Cloud Points

The cloud points of the prepared nonionic surfactants the increase of the hydrophobic and hydrophilic parts causes the rise of the cloud point. EO9 in each series with hydrophobic part at C_{12} are the highest one over all series. This increase may attribute the increase of the hydration of the oxygen in ethylene oxide, and the increased ethylene oxide chain length needs higher temperatures until phase separation occurs (Hussein, 2010).

Foaming Power

Nonionic surfactants are known for their low foam production, where the foam height increases with the increasing of the ethylene oxide units and chain length of hydrocarbon part per molecule of the surfactant (Sallay et al., 1997). From Table 5 it can be seen that the prepared compounds have moderated foaming power, and each compound exhibits not only moderate foam production but also low-foaming stability. These effects may be due to the hydrophobic part (containing a chain and a ring) and the imide group in the molecules. Consequently, an increase in the size of the molecule will lead to a small cohesive force being produced at the surface (Mohamed et al., 2005).

Wetting Time

It is clear from Table 5 that all the synthesized surfactants show a small wetting time but a slight increase in the wetting time is recorded with a low number of ethylene oxide units (Cohen and Rosen, 1981).

Biodegradability

The ST data listed in Table 6, since the prepared nonionic surfactants $(4–6)_{a–c}$ under investigation have different hydrophilic and hydrophobic parts, both parts affect the biodegradation process. It is clear from the data in Table 8 that the biodegradation has a good degradability ratio for the prepared compounds, ranging between 50% and 99% after the eighth day.

ST at the CMC

For the prepared nonionic surfactants $(4–6)_{a–c}$ the ST values depend mainly on the hydrophobic part. The values of ST at the CMC for these compounds decreased by increasing their number of methylene units (Graciaa et al., 1983). The CMC and surface parameters for the products obtained from the constricted relationship of the ST (γ) *versus* the negative logarithm of concentration, as indicated in Figs 2–4 for $(4–6)_{a–c}$ of the synthesized nonionic surfactants. The CMC values, as shown in Table 7, range between 7.9×10^{-3} and 3.61×10^{-3} of nonionic surfactants, semiliterate of CMC in the first three compounds due to SAR (structure activity relationships) because all of them C_8 i.e. the external tail of alkyl chain same so hydrophobicity for them also approximately same. Transformed from C_8 to C_{10} in the fourth compound as a regular increase in chain length which has very little effect on hydrophobicity so the difference between CMC values is very low. Generally, the synthesized surfactant molecules showed consistent behavior according to their hydrophobic part. The CMCs of the nonionic $(4–6)_{a–c}$ surfactants are low, which may be due to the presence of ester and imide groups besides the ethylene oxide units, which produce molecules that are multifunctional (i.e., have low CMC and high solubilizing capacity (Zhu et al., 1992). Ottaviani et al. (2015) reported an inverse relation between the log solubility of the surfactant molecules and their log CMC values. This is because the surfactant molecules in the surfactant solution take four states: present at surface, in the form of micelle, free in the bulk or adsorbed at the wall of solution container. Thus, when the solubility of the surfactant molecules increases, there are more surfactant molecules present in the bulk of the solution than at the surface so the critical concentration at which micelles formed decreases.

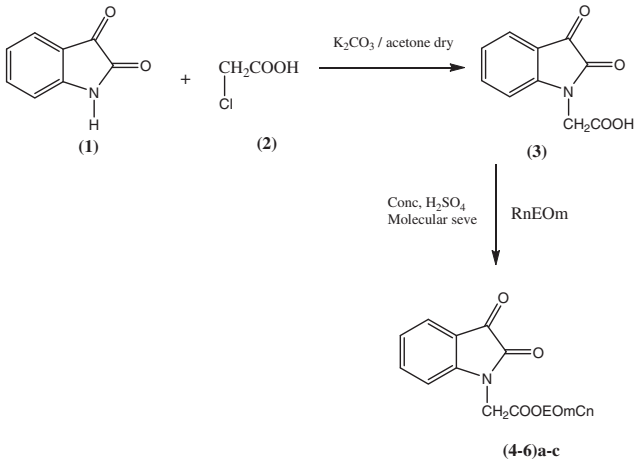

Scheme 1 The prepared compounds
where n = 8–12 (octyl C_8; decyl C_{10}, and dodecyl C_{12} of the alkyl chains, respectively, and m = 5, 7 and 9 units of ethylene glycol, respectively

Compound	Abbreviation	Molecular structure
N-isatin-$EO_{9\text{-}5)}$-C_8		
4_a	*N*-isatin-EO_5-C_8	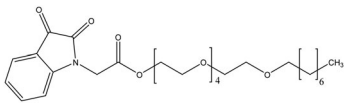
4_b	*N*-isatin-EO_7-C_8	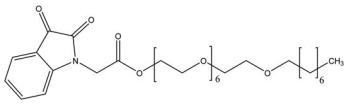
4_c	*N*-isatin-EO_9-C_8	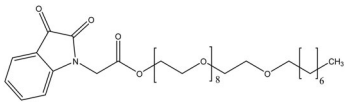
N-isatin-$EO_{(5–9)}$-C_{10}		
5_a	*N*-isatin-EO_5-C_{10}	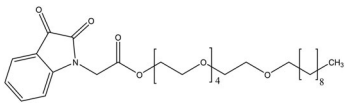
5_b	*N*-isatin-EO_7-C_{10}	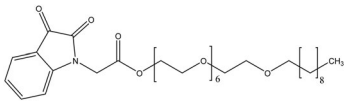
5_c	*N*-isatin-EO_9-C_{10}	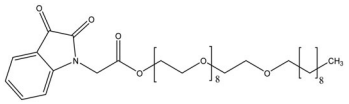
N-isatin-$EO_{(5–9)}$-C_{12}		
6_a	*N*-isatin-EO_5-C_{12}	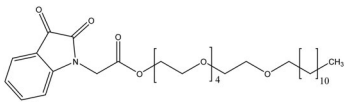
6_b	*N*-isatin-EO_7-C_{12}	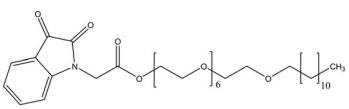
6_c	*N*-isatin-EO_9-C_{12}	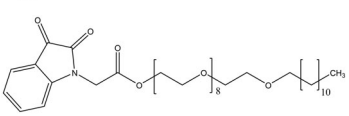

Table 3 FTIR data for *N*-isatin-$EO_{5,7,9}$-$C_{8,10,12}$

Compound	ν_{OH}	ν_{CH} aliphatic	$\nu_{C=O}$	Glycol
$\mathbf{4_a}$	3400	2925–2873	1700–1705	–
$\mathbf{4_b}$	–	2874	1741, 1462.74	1140
$\mathbf{4_c}$	–	1462, 2873.42 cm	1741, 1619.91	1146
$\mathbf{5_a}$	–	2925.48, 1458.89	1735.62, 1622.8	1067
$\mathbf{5_b}$	–	2922	1619, 1739	1070
$\mathbf{5_c}$	–	1458, 2922	1616, 1734	1102
$\mathbf{6_a}$	–	1468, 2886	1619, 1740	1114
$\mathbf{6_b}$	–	1462, 2873	1618, 1743	1106
$\mathbf{6_c}$	–	1401, 2922	1617, 1735	1093

Effectiveness

From the data in Table 7 the prepared nonionic surfactants demonstrate a good effect in reducing the ST at the CMC (Mousli and Tazerouti, 2011).

Efficiency

From Table 7 it can be seen that an increase in the hydrophobic part leads to an increase in efficiency. Increasing the chain length increases the hydrophobicity of the molecules.

Table 4 H^1NMR data for *N*-isatin-$EO_{5,7,9}$-$C_{8,10,12}$

Compd. no.	
$\mathbf{4_a}$	δ_{ppm} at 0.762 (t, 3H of terminal $\underline{CH_3}$–$(CH_2)_7$–); δ_{ppm} at 1.201–1.502 (m, 12H of CH_3–$\underline{(CH_2)_6}$–CH_2–O); δ_{ppm} at 3.356–3.401 (t, 2H of CH_3–$(CH2)_6$–$\underline{CH_2}$–O); δ_{ppm} at 3.522–3.806 (m, 18H of –$COOCH_2\underline{CH_2O(CH_2CH_2O)_4}$–$OCH_2$)–; δ_{ppm} at 3.806–4.057 (t, 2H of –$COO\underline{CH_2}CH_2O$); δ_{ppm} at 4.732 (s, 2H of N–$\underline{CH_2}CO$); δ_{ppm} at 6.926–7.430 (m, 4H of aromatic protons)
$\mathbf{4_b}$	δ_{ppm} at 0.812 (t, 3H of terminal $\underline{CH_3}$–$(CH_2)_7$–); δ_{ppm} at 1.206–1.507 (m, 12H of CH_3–$\underline{(CH_2)_6}$–CH_2–O); δ_{ppm} at 3.364–3.385 (t, 2H of CH_3–$(CH2)_6$–$\underline{CH_2}$–O); δ_{ppm} at 3.408–3.582 (m, 26H of –$COOCH_2\underline{CH_2O(CH_2CH_2O)_6}$–$OCH_2$)–; δ_{ppm} at 3.815–4.016 (t, 2H of –$COO\underline{CH_2}CH_2O$); δ_{ppm} at 4.358 (s, 2H of N–$\underline{CH_2}CO$); δ_{ppm} at 6.959–7.504 (m, 4H of aromatic protons)
$\mathbf{5_b}$	δ_{ppm} at 0.856–0.877 (t, 3H of terminal $\underline{CH_3}$–$(CH_2)_8$–); δ_{ppm} at 1.254 (m, 16H of CH_3–$\underline{(CH_2)_8}$–CH_2–O); δ_{ppm} at 3.445 (t, 2H of CH_3–$(CH2)_6$–$\underline{CH_2}$–O); δ_{ppm}at 3.466–3.650 (m, 26H of –$COOCH_2\underline{CH_2O(CH_2CH_2O)_6}$–$OCH_2$)–; δ_{ppm} at 3.740 (t, 2H of –$COO\underline{CH_2}CH_2O$); δ_{ppm} at 4.103 (s, 2H of N–$\underline{CH_2}CO$); δ_{ppm} at 6.949–7.617 (m, 4H of aromatic protons)
$\mathbf{5_c}$	δ_{ppm} at 0.89 (t, 3H of terminal $\underline{CH_3}$–$(CH_2)_8$–); δ_{ppm} at 1.240 (m, 16H of CH_3–$\underline{(CH_2)_8}$–CH_2–O); δ_{ppm} at 3.577 (t, 2H of CH_3–$(CH2)_6$–$\underline{CH_2}$–O); δ_{ppm}at 3.691–3.706 (m, 34H of –$COOCH_2\underline{CH_2O(CH_2CH_2O)_8}$–$OCH_2$)–; δ_{ppm} at 3.720 (t, 2H of –$COO\underline{CH_2}CH_2O$); δ_{ppm} at 4.072 (s, 2H of N–$\underline{CH_2}CO$); δ_{ppm} at 6.928–7.273 (m, 4H of aromatic protons)

Table 5 Surface properties of synthesized nonionic surfactants (*N*-isatin-$EO_{5,7,9}$-$C_{8,10,12}$)

Compound	Cloud point (°C 1.0 wt%)	Foaming 0.1 wt%		Foaming power (%)	Witting time (s 0.1 wt%)
		Initial foam (mm)	After 5 min. (mm)		
$\mathbf{4_a}$	60	25	20	80.0	91
$\mathbf{4_b}$	71	28	23	82.0	94
$\mathbf{4_c}$	80	34	28	82.4	96
$\mathbf{5_a}$	80	26	21	80.8	95
$\mathbf{5_b}$	85	30	25	83.3	97
$\mathbf{5_c}$	90	35	29	82.9	100
$\mathbf{6_a}$	80	32	26	81.3	112
$\mathbf{6_b}$	90	36	30	83.3	114
$\mathbf{6_c}$	>100	38	32	84.2	116
Marlipal 24/50 ethoxylate[a]	22	—	—	100	20

[a] Marlipal 24/50 ethoxylate is a commonly used nonionic surfactant prepared from decyl fatty alcohol and 7 mol of ethylene oxide.

Table 6 Biodegradability of synthesized nonionic surfactants (*N*-isatin-$EO_{5\text{-}9}$-$C_{8,10,12}$)

Compound	1st day	2nd day	3rd day	4th day	5th day	6th day	7th day	8th day
$\mathbf{4_a}$	55	60	72	80	88	96	–	–
$\mathbf{4_b}$	55	62	73	79	91	98	–	–
$\mathbf{4_c}$	56	64	75	82	93	97	99	–
$\mathbf{5_a}$	53	60	68	76	86	90	97	–
$\mathbf{5_b}$	52	68	65	81	84	92	96	97
$\mathbf{5_c}$	51	56	64	71	79	86	92	96
$\mathbf{6_a}$	52	61	70	78	85	94	98	–
$\mathbf{6_b}$	51	59	67	77	84	93	98	–
$\mathbf{6_c}$	50	56	65	73	84	90	94	97

Table 7 Surface activity of isatin nonionic surfactants (*N*-isatin-$EO_{5\text{-}9}$-C_{8-12})

Compound	cmc	π_{cmc}	pc20	Γ_{max}	A_{min} (nm^2)
$\mathbf{4_a}$	8.79E−03	37.00	4.59	9.12E−11	1.82
$\mathbf{4_b}$	7.94E−03	36.23	4.30	9.64E−11	1.72
$\mathbf{4_c}$	6.85E−03	34.69	4.09	9.68E−11	1.72
$\mathbf{5_a}$	6.78E−03	36.07	4.44	8.93E−11	1.86
$\mathbf{5_b}$	6.11E−03	35.85	4.16	9.81E−11	1.69
$\mathbf{5_c}$	5.73E−03	34.31	4.13	1.00E−10	1.66
$\mathbf{6_a}$	5.41E−03	35.85	4.63	9.03E−11	1.84
$\mathbf{6_b}$	5.01E−03	35.46	4.00	1.01E−10	1.64
$\mathbf{6_c}$	4.40E−03	33.82	3.84	1.07E−10	1.55

Hence, hydrophobic interactions increase, which leads to the migration of molecules to the surface, reducing the ST and increasing the efficiency (El-Sukkary et al., 2010).

Maximum Surface Excess

The data in Table 7 show that the migration of a large number of molecules on the interface due to the increasing hydrophobic character of the surfactant products increases the Γ_{max} (El-Sukkary et al., 2010).

Minimum Surface Area

The data in Table 7 indicate that an increase in Γ_{max} values leads to an increase in the number of adsorbed surfactant molecules at the interface, which leads to decrease in A_{min} values.

Computational Study

To achieve a better understanding of the molecular properties of the studied compounds and conformational analyses performed on the crystal structures. Geometrical optimization of the ligand structure exhibited a common feature for compounds 4_{a-c} and 5_c in Tables S1–S3 and Fig. 5. The computed molecular parameters, total energy, electronic energy, heat of formation, highest occupied molecular orbital (HOMO) energies, lowest unoccupied molecular orbital (LUMO) energies, and dipole moment for compounds $\mathbf{5_{a-c}}$ are listed in Table 8. The low calculated

Table 8 The optimized calculations energies for nonionic surfactants 5_{a-c}

Compound	E	HF	IP	HOMO	LUMO	HBD	HBA	Log*P*	*V*	TPSA	%*A*BS	Log *S*	Δ*E*
$\mathbf{5_a}$	−134, 034.73	−168.80	8.96	−8.96	−1.09	2	7	2.63	0	101.93	73.83	−4.67	8.39
$\mathbf{5_b}$	−130, 228.95	−121.66	9.16	−9.16	−0.87	3	10	1.88	0	139.89	60.73	−5.45	8.29
$\mathbf{5_c}$	−137, 635.72	−183.02	9.07	−9.03	−1.21	3	8	4.80	0	141.34	60.24	−6.64	7.50

log *P*, calculated lipophilicity; log *S*, solubility parameter; HBA, number of hydrogen bond acceptors; HBD, number of hydrogen bond donors; *V*, volume ($Å^3$).

Table 9 Biological activities of the prepared nonionic surfactants (*N*-isatin-EO_{5-9}-C_{8-12})

	Inhibition zone diameter (mm l mg sample)			
	Escherichia coli (G −ve)	*Staphylococcus aureus* (G +ve)	*Aspergillus flavus* fungus	*Candida albicans* fungus
	30	31	—	—
	—	—	17	19
Compound	Nonionic surfactants			
$\mathbf{4_a}$	20	26	12	11
$\mathbf{4_b}$	22	23	11	11
$\mathbf{4_c}$	24	25	13	10
$\mathbf{5_a}$	19	25	11	10
$\mathbf{5_b}$	20	23	15	11
$\mathbf{5_c}$	19	19	14	12
$\mathbf{6_a}$	21	25	12	13
$\mathbf{6_b}$	21	27	16	11
$\mathbf{6_c}$	26	29	15	11

Table 10 Docking energy scores (kcal/mol) derived from MOE tool for $\mathbf{4_{a,b}}$, $\mathbf{5_{a,b}}$, and $\mathbf{6_{a,c}}$

Compound	Δ*G*	Int.	HB	E_{ele}	E_{vdw}	Δ*G*
$\mathbf{4_a}$	−5.7810	5.484	89.771	−48.661	−10.347	−20.786
$\mathbf{4_b}$	−7.073	3.179	106.88	−86.77	−11.151	−24.88
$\mathbf{5_a}$	−6.879	2.667	92.28	−42.03	−11.176	−24.54
$\mathbf{5_b}$	−6.975	3.703	115.1	−78.21	−11.678	−24.93
$\mathbf{6_a}$	−6.498	1.937	93.62	−79.25	−10.331	−20.74
$\mathbf{6_c}$	−6.768	6.385	139.4	−24.68	−10.688	−16.43

Δ*G*, free binding energy of the ligand from a given conformer; Int., affinity binding energy of hydrogen bond interaction with receptor; HB, hydrogen bonding energy between protein and ligand; E_{ele}, electrostatic interaction with the receptor; E_{vdw}, van der Waals energies between the ligand and the receptor.

energies and high HOMO energy values show that the molecules are good electron donors. On other hand, the lower HOMO energy values indicate a weaker ability of the molecules to donate electrons. The LUMO energy shows the ability of a molecule to receive electrons, which explains the potency of the antimicrobial activity.

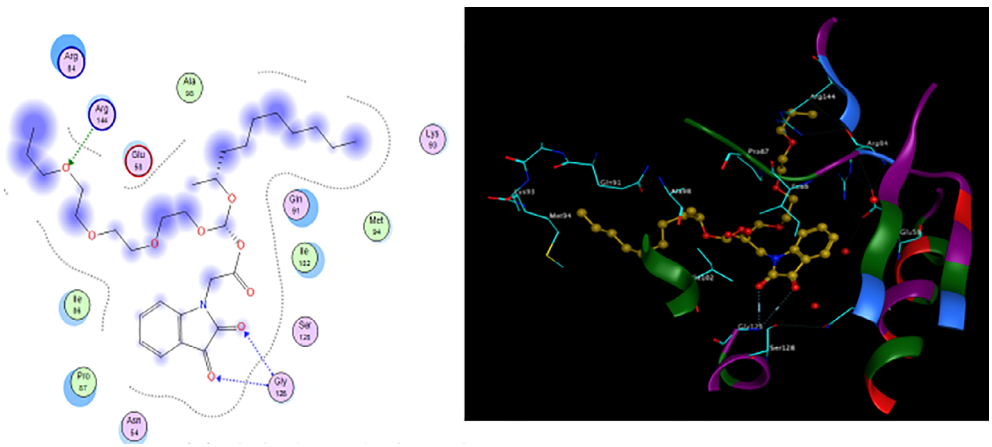

Fig. 6 The binding mode of 5_a in active DNA gyrase

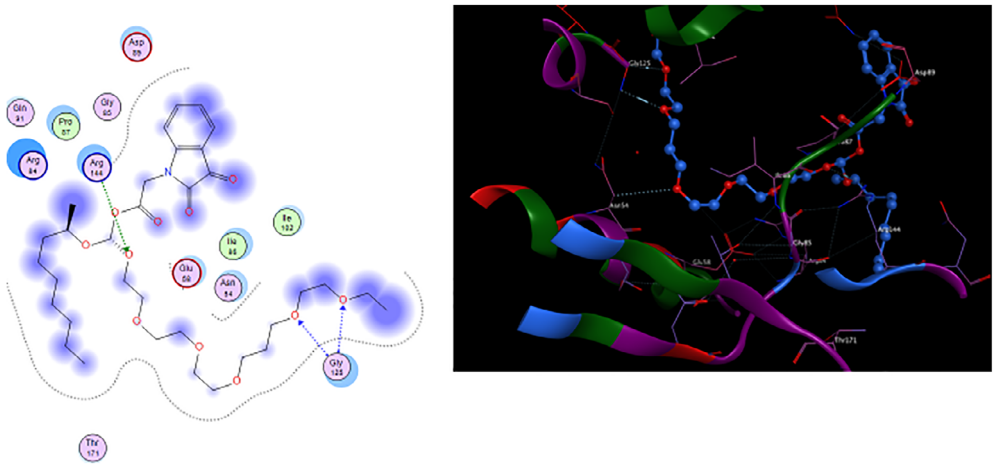

Fig. 7 The binding mode of 5_b in active DNA gyrase

ADMET Profiling

Many potential therapeutic agents fail to reach the clinic because of their ADMET properties. ADMET profiling performed for compounds $\mathbf{5_{a–c}}$ are listed in Table 8 by the determination of the topological polar surface area (TPSA), absorption percent (%ABS) (Zhao et al., 2002), and five rules (Lipinski, 1997). Our results reveal that the *C* log *P* (factor of the lipophilicity) is less than 5.0, the hydrogen bond acceptors are between 7 and 10, and the hydrogen bond donors are between 1 and 5. These data show that these compounds fulfill Lipinski's rule, and the absorption percentage ranges between ~50% and 86%. Oral bioavailability plays an important role in the development of bioactive molecules as therapeutic agents.

Biological Activity

The cell membrane of microorganisms contain lipids, which by its role gained it hydrophobic property, surfactant molecules when adsorbed at the water cell membrane increases its hydrophobicity, which increases its permeability toward the outside media. This disturbs the biological interactions, reducing the biological activity of DNA and cell cytoplasm (Hussein and Khowdiary, 2014). All the prepared nonionic $(4–6)_{a–c}$ surfactants were screened for their antimicrobial activities. To study the antibacterial and antifungal properties, the microorganisms employed were *Staphylococcus aureus* (G^-), *Escherichia coli* (G^+), *Candida albicans* (fungus), and *A. flavus* fungus. From the results in Table 9, it can be seen that product $\mathbf{6_c}$ is the most active compound against both type Bactria (G^+ and G^-), while compound $\mathbf{6_b}$ the most potency *via Aspergillus flavus* fungus. Compound $\mathbf{6_a}$ is the most effective against *Candida albicans* fungus. In addition, all synthesized compounds exhibited lower potency compared with the reference drug. Generally, surfactants are able to show antimicrobial activity against bacteria and fungi (Kofonow and Adappa, 2012). This activity comes from the fact that in this nonionic surfactant, A_{min} values are very low, which means that adsorption increases at the cell membrane MOE and thus an increase in biological activity occurs.

Docking Studies

The docking study targeted DNA gyrase and cathepsin B to examine a mode of action of the small compounds as antimicrobial and antitumor agents, respectively. The ligand–protein interaction behavior estimated based on docking score function as implemented in MOE 2015. All calculations for the docking experiment were carried out as reported earlier (Elhenawy et al., 2015; Elhenawy et al., 2019b, b) and are presented in Table 10. The crystal structures DNA gyrase (PDB: 4uro (Robb et al., 2013) obtained. The compounds $\mathbf{4_{a,b}}$, $\mathbf{5_{a,b}}$, and $\mathbf{6_{a,c}}$ dock into active sites on the receptors. The ligands form complexes with the active sites of both active site of enzymes. The extracted docked poses of ligands energy-minimized with molecular mechanics (Amber12: EHT) force field, until the gradient convergence reached 0.05 kcal mol^{-1}. The highest MOE scoring function for the tested compounds was applied to evaluate the binding affinities of the tested compounds (Table 10). The compounds $\mathbf{4_{a,b}}$, $\mathbf{5_{a,b}}$, and $\mathbf{6_{a,c}}$ exhibited binding affinity with DNA gyrase (−5.7810 to −7.073 kcal mol^{-1}) (Table 10). The tested compounds also combined with the important amino acid residue Gly125 for DNA gyrase active site, which there formed a strong hydrogen bonds with equal bond distances about 2.9° (Figs 6 and 7, and Table 10). These compounds were arranged parallel to Gly125 which there are hydrophilic key for stabilization these compounds in receptor. The different interaction modes of ligands with hydrophilic amino acids backbone in both binding sites 4uro

(Figs 6 and 7) postulated that hydrophobicity and membrane permeability are important pharmabiotic characteristics for absorption molecules in biological system.

Conflict of Interest The authors declare that they have no conflict of interest.

References

Ahmed, M., Sallay, P., Rusznak, I., & Farkas, L. (1996) Determination of the average ethoxylation degree. *Tenside Surfactants Detergents*, **33**:410–411.

Albright, J. D., Moran, D. B., Wright, W. B., Collins, J. B., Beer, B., Lippa, A. S., & Greenblatt, E. N. (1981) Synthesis and anxiolytic activity of 6-(substituted-phenyl)-1,2,4-triazolo [4,3-b] pyridazines. *Journal of Medicinal Chemistry*, **24**:592–600. https://doi.org/10.1021/jm00137a020

Arief, M., Ahmed, M., Said, A., & Selim, N. (2013) Synthesis of some heterocyclic compounds based on (2,3-dioxo-2,3-dihydro-1H-indol-1-yl) acetyl acetic acid derivatives. *Journal of Basic and Applied Sciences*, **2**:153. https://doi.org/10.14419/ijbas.v2i2.721

Bauer, A., Kirby, W., Sherris, J. C., & Turck, M. (1966) Antibiotic susceptibility testing by a standardized single disk method. *American Journal of Clinical Pathology*, **45**:493–496. https://doi.org/10.1093/ajcp/45.4_ts.493

Chavda, S., Bahadur, P., & Aswal, V. K. (2011) Interaction between nonionic and gemini (cationic) surfactants: Effect of spacer chain length. *Journal of Surfactants and Detergents*, **14**:353–362. https://doi.org/10.1007/s11743-011-1263-6

Chen, L. R., Wang, Y. C., Lin, Y. W., Chou, S. Y., & Chen, S. F. (2005) Synthesis and evaluation of isatin derivatives as effective SARS coronavirus 3CLprotease inhibitors. *Bioorganic & Medicinal Chemistry Letters*, **15**:3058–3062. https://doi.org/10.1016/j.bmcl.2005.04.027

Cohen, A., & Rosen, M. (1981) Wetting properties of nonionic surfactants of homogeneous structure C_{12} H_{25} $(OC_2$ $H_4)_x$ OH. *Journal of the American Oil Chemists' Society*, **58**:1062–1066. https://doi.org/10.1007/BF02679327

Cress, J. (1987) *Nonionic surfactants* (Vol. **19**, pp. 10–25). New York, NY: Marcel Dekker.

Durham, K. (1961) *Surface activity and detergency* (pp. 158–192). MacMillan.

Elhenawy, A. A., AL-Harbi, L. M., El-Gazzar, M. A., Khowdiary, M. M., Ouidate, A., & Salim, A. (2019b) *Biomedicine & Pharmacotherapy*, **116**:109024–109036. https://doi.org/10.1016/j.biopha.2019.109024

El-Sukkary, M., Aiad, I., Deeb, A., El-Awady, M., Ahmed, H., & Shaban, S. (2010) Preparation and characterization of some novel quaternary ammonium salts based on schiff-base as a corrosion inhibitor. *Petroleum Science and Technology*, **28**:1158–1169. https://doi.org/10.1080/10916460902967718

Geng, X. F., Hu, X. Q., Xia, J. J., & Jia, X. C. (2013) Synthesis and surface activities of a novel di-hydroxyl-sulfate-betaine-type zwitterionic gemini surfactants. *Applied Surface Science*, **271**:284–290. https://doi.org/10.1016/j.apsusc.2013.01.185

Graciaa, A., Lachaise, J., Sayous, J., Grenier, P., Yiv, S., Schechter, R., & Wade, W. (1983) The partitioning of complex surfactant mixtures between oil/water/microemulsion phases at high surfactant concentrations. *Journal of Colloid and Interface Science*, **93**:474–486. https://doi.org/10.1016/0021-9797(83)90431-9

Halgren, T. A. (1996) Merck molecular force field basis, form, scope, parameterization, and performance of MMFF94. *Journal of Computational Chemistry*, **17**:490–519. https://doi.org/10.1002/(SICI)1096-987X(199604)17:5/6<490::AID-JCC1>3.0.CO;2-P

Hussein, A. M. (2010) Preparation and evaluation of sulphonamide nonionic surfactants. *Grasas y Aceites*, **61**:7–15. https://doi.org/10.3989/gya.053509

Hussein, A. M., & Khowdiary, M. M. (2014) Synthesis quantum chemical calculations and properties of nonionic and nonionic–anionic surfactants based on fatty alkyl succinate. *Journal of Surfactants and Detergents*, **17**:615–627. https://doi.org/10.1007/s11743-014-1568-3

Jancevska, M. B., & Stojceva, G. H. (1975) Naproxenyl amino acid derivatives: Design, synthesis,docking, QSAR and anti-inflammatory and analgesic activity. *Technol Makedonija*, **2**:53 (CA, 87: 184309h).

Jarrahpour, A., Khalili, D., De-Clercq, E., Salmi, C., & Brunel, J. M. (2007) Synthesis, antibacterial, antifungal and antiviral activity evaluation of some new bis-Schiff bases of isatin and their derivatives. *Molecules*, **12**:1720–1730. https://doi.org/10.3390/12081720

Jays, J., Rochani, A., Kumar, A., Suma, B. V., Venkataramana, C., & Madhavan, V. (2011) In silico ADME and toxicity studies of some synthesized novel isatin derivatives. *Journal of Pharmacy & Bioallied Sciences*, **2**:25–33.

Kofonow, J. M., & Adappa, N. D. (2012) In vitro antimicrobial activity of SinuSurf. *Journal of Oto-rhino-laryngology and Its Related Specialities*, **74**:179–184. https://doi.org/10.1159/000339585

Liebowitz, L. D., Ashbee, H. R., Evans, E. G., Chong, Y., Mallatova, N. M., & Zaidi, D. (2001) Gibbs and global antifungal surveillance group, two year global evaluation of the susceptibility of Candida species to fluconazole by disk diffusion. *Diagnostic Microbiology and Infectious Disease*, **4**:27–33. https://doi.org/10.1016/S0732-8893(01)00243-7

Lipinski, C. A., Lombardo, F., Dominy, B. W., & Feeney, P. J. (1997) Experimental and computational approaches to estimate solubility and permeability in drug discovery and development settings. *Advanced Drug Delivery Reviews*, **23**:3–25. https://doi.org/10.1016/S0169-409X(96)00423-1

Mohamed, M. Z., Ismail, D. A., & Mohamed, A. S. (2005) Synthesis and evaluation of new amphiphilic polyethylene glycol-based triblock copolymer surfactants. *Journal of Surfactants and Detergents*, **8**:175–180. https://doi.org/10.1007/s11743-005-344-4

Molecular Operating Environment (MOE). (2017) C.C.G.U., 1010 handbook, Montreal, QC, Canada.

Mousli, R., & Tazerouti, A. (2011) Synthesis and some surface properties of glycine-based surfactants. *Journal of Surfactants and Detergents*, **14**:65–72. https://doi.org/10.1007/s11743-010-1210-y

Ottaviani, G., Wendelspiess, S., & Alvarez-Sanchez, R. (2015) Importance of critical micellar concentration for the prediction of solubility enhancement in biorelevant media. *Journal of Molecular Pharmaceutics*, **12**:1171–1179. https://doi.org/10.1021/mp5006992

Pegiadou-Koemtjopoulou, S., Tsatsaroni, E., & Mylona, M. (1998) Pyrimidinium cationic surfactants as emulsifiers for oil-in-water emulsions. *Journal of Surfactants and Detergents*, **1**:499–502.

Pfaller, M. A., Burmeister, L., Bartlett, M., & Rinaldi, M. (1988) Multicenter evaluation of four methods of yeast inoculum preparation. *Journal of Clinical Microbiology*, **26**:1437–1441.

Robb, M., Cheeseman, J., Scalmani, G., Barone, V., Mennucci, B., & Petersson, G. (2013) Gaussian 09, Revision D. 01, Gaussian, Inc., Wallingford CT. Gaussian 09, Revision D01. Gaussian. Inc., Wallingford CT Google Scholar.

Saito, Y., Sato, T., & Anazawa, I. (1989) Correlation between distribution of oxyethylene chain and physicochemical properties of nonionic surfactants. *Yakuzaigaku*, **49**:180–183.

Sallay, P., Bekassy, S., Ahmed, M. H., Farkas, L., & Rusznak, I. (1997) A novel way for hydroxyethylation by using clay catalysts. *Tetrahedron Letters*, **38**:661–664. https://doi.org/10.1016/S0040-4039(96)02386-6

Takeshita, T., Shimohara, T., & Maeda, S. (1982) Synthesis of EDTA monoalkyl amide chelates and evaluation of the surface-active properties. *Journal of the American Chemical Society*, **59**:104–107. https://doi.org/10.1007/BF02678725

Zhao, Y. H., Abraham, M. H., Le, J., Hersey, A., Luscombe, C. N., Beck, G., … Cooper, I. (2002) Rate-limited steps of human oral absorption and QSAR studies. *Pharmaceutical Research*, **19**: 1446–1457.

Zhu, Y. P., Masuyama, A., Kirito, Y. I., Okahara, M., & Rosen, M. J. (1992) Preparation and properties of glycerol-based double-or triple-chain surfactants with two hydrophilic ionic groups. *Journal of the American Oil Chemists Society*, **69**:626–632.

Biographies

Ahmed M. Hussein was awarded his Ph.D. from the Technical University of Budapest, Hungary, in field of surfactants. He is associated professor at the Faculty of Science, Benha University, Egypt. His research work is in the synthesis and evaluation of surfactants. He now works at the Faculty of Science, Jazan University, Saudi Arabia.

Manal M. Khowdiary is a researcher in the petrochemicals department at the Egyptian Petroleum Research Institute. Her interests are the synthesis and evaluation of surfactants in several applications, including detergency and biocidal activity.